Received: 18 November 2023 | Revised: 18 April 2024 | Accepted: 30 April 2024

IET Power Electronics

DOI: 10.1049/pel2.12723

The Institution of Engineering and Technology WILEY

ORIGINAL RESEARCH

Optimization of battery/ultra-capacitor hybrid energy storage system for frequency response support in low-inertia microgrid

Philemon Yegon[1,2] | **Mukhtiar Singh**[1]

[1]Department of Electrical Engineering, Delhi Technological University, Delhi, India

[2]Department of Electrical and Electronic Engineering, Kenyatta University, Nairobi, Kenya

Correspondence
Philemon Yegon, Department of Electrical and Electronic Engineering, Kenyatta University, P.O Box 43844-00100, Nairobi, Kenya.
Email: yegon.philemon@ku.ac.ke

Abstract

Modern power system networks are under statutory obligations to integrate renewable energy sources (RES). The primary reason is to meet ever-increasing energy demand and also to curtail environmental pollution by greenhouse gases. However, the higher penetration of RES has the tendency of reducing inertia of overall power system network. Consequently, frequency stability is affected and deviates beyond allowable permissible limits leading to power blackouts, load shedding, and even total system failure. To address the issues associated with reduced inertia, an optimal control of hybrid energy storage system (HESS) has been proposed. HESS is basically a combination of battery and ultracapacitor, where ultracapacitor addresses rapidly varying power component by mimicking inertia while the battery compensates long-term power variations. Thus, the HESS is effectively controlled to compensate the loss of inertia by regulating its energy flow. For the purpose of improved efficiency and better power management of the HESS, an improvised particle swarm optimization (MPSO)-based virtual inertia control design has been proposed. The proposed MPSO is utilized to tune the gains of bidirectional dc–dc converter in such a way that improves frequency nadir with faster response to transient disturbances. This proposed method is simulated in MATLAB and its merits are validated in real time using hardware in loop. On analysing of the results, it can be observed that frequency nadir is improved by 48.96% with significant reduction in rate of change of frequency in comparison to conventional particle swarm optimization.

1 | INTRODUCTION

In modern times, the energy industry has seen significant growth. Several countries around the world are facing the challenge of ever-increasing energy demand. The conventional methods of power generation are already at their peak and going to be exhausted in near future. Additionally, the traditional methods of power generation are environmentally hazardous. Fossil fuels generate greenhouse gases, which contaminate the environment and pose a threat to the living organisms inhabiting the region. In order to address these issues, renewable energy sources (RES) are being rapidly implemented in contemporary power system networks. Nevertheless, the growing integration of power electronics interfaced RES results into reduced inertia and hence, poses a significant challenge for the grid stability [1]. The reduced inertia triggers frequency instability (high rate of change of frequency (RoCoF), frequency nadir and zenith). Further, this problem is very much exaggerated in power system network confined to small geographical locations termed as microgrid.

The inertia issue in microgrid operation and control is of lot of concern and several schemes primarily based on rotational mass have been proposed. Synchronous generators operating without any load, commonly referred to as synchronous

Abbreviations: AM, analytical methods; DG, distributed generation system; FAESS and SAESS, fast-acting and slow acting energy storage system; FFR, fast frequency response; GHG, greenhouse gas; HESS, hybrid energy storage system; IGBT, insulated-gate bipolar transistor; KNDGC, Kenya National Grid Distribution Code; MG, microgrid; MPSO, improvised particle swarm optimization; NERC, North American Electric Reliability Corporation; PAM, Pinch analysis method; PID, proportional (Kp), integral (Ki), and derivative (Kd) controller; PSO, particle swarm optimization technique; PTS, power transformation system; PWM, pulse width modulation; RES, renewable energy sources; RoCoF, rate of change of frequency; RPM, Ragone plot method; SBM, search-based methods; SM, statistical methods; SOC, state of charge; VFOPID, variable fractional order PID; VSG, virtual synchronous generators; VSMs, virtual synchronous machines.

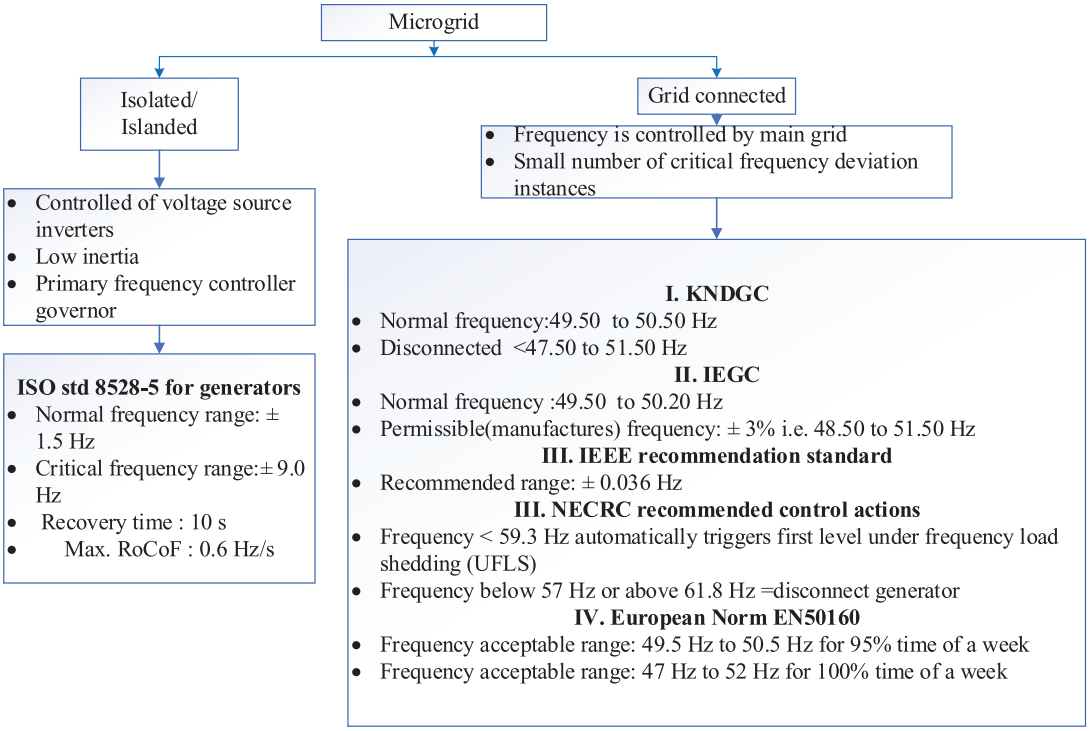

FIGURE 1 Frequency standards of microgrid [4, 5].

condensers (SC), have been widely used to compensate the loss of inertia [2]. However, the use of dedicated synchronous condenser is bulky, inefficient, and costly affair without any significant improvement in performance. To reduce the additional burden of machine, recently few schemes have been proposed where the inertia of rotating wind turbines is utilised as SC [3]. While this kind of technology seems very promising, but under variable speed operation of wind turbines, it becomes very difficult to extract the characteristics of typical SC and hence, not suitable for inertial control. The energy stored inside DC-link capacitors is also found to be very useful to overcome small transient load disturbances, but it has very limited capability heavily dependent on the size of the capacitor. Further, this kind of approach is suitable only where slight variation in DC-link voltage is allowed and not applicable to rigid DC-links comprising batteries having almost fixed voltages. Sometimes, the generating facilities in a microgrid are operated under partial-loading to keep a cushion for further increase in load. However, running a microgrid under reduced loading is extremely inefficient and increases the per unit cost of generating electricity.

Figure 1 shows frequency codes for restoration in microgrid operation prevalent in various organizations and countries.

Very recently, the energy storage systems (ESS) have been discussed widely with the intention of solving the problem of frequency instability in distributed generation system (DG) [6]. The ESS is found to be most promising for virtual synchronous machine emulation in power electronics dominant RES-based power generation. ESS having limited capacity in terms of both power and energy can be categorized on the basis of their response; rapid response ESS like flywheel, ultra-capacitors and li-ion batteries are called short-term while chemical battery (lead acid), pumped hydro storage and compressed air are known as long-term ESS. Most of the research work reported in the area of ESS power management is limited to theoretical analysis in control stability of droop, but silent about optimal sizing of ESS [7, 8]. Optimal sizing of Hybrid ESS is one of the essential ingredients not limited only to cost effectiveness but also to achieve enhanced performance out of it. Further, it is also necessary to maintain state of charge (SOC) within a given acceptable level and that is why it needs to be included in feedback control loop [9, 10]. Chu Sun proposed feedback control with additional Proportional and Integral (PI) regulator for fast-acting and slow acting energy storage system (FAESS and SAESS) to emulate synchronous generator [11]. However, in this proposal the design of PI parameters is done through the trial-and-error method. The challenge of optimal energy control was addressed by *Spyridon Chapaloglou* in [12] by controlling primary frequency through optimal methods. But, the sizing aspect of ESS is not considered in this particular article. In [13, 14], PV-battery energy storage system (BESS) is proposed and optimized using linear programming, but it did not explain effectiveness of hierarchical control nature of the systems [15, 16].

Recently, HESS-based energy management techniques have been proposed to address the inertia issue. Through the hybridization of a battery and an ultra-capacitor, fast frequency response (FFR) is achieved [17]. Inertia and damping emulation are restored using the energy recovered from them. Ultra-capacitor has high specific power density; hence, its response

time is rapid, that is why it is also referred to as rapid response energy storage system (RRESS). The battery has high energy density; hence, the response is slow and termed slow response energy storage system (SRESS). The idea of virtual synchronous generators (VSGs) replicated by power electronic converters is becoming increasingly popular [18]. However, problems with response time and parameter fluctuations make overall control more complex. Numerous studies have been examined to analyse the non-inertia generation effect on frequency dependability, resilience, and stability of bulk power networks [19]. In [20], the ESS has been regulated for emulating the characteristics of VSG to maintain frequency stability in low-inertia network. A typical VSG control approach incorporates the droop control loops to regulate its output active and reactive power for the better terminal voltage regulation and faster inertial response. However, sizing of HESS and determining the gains of control loops for different operating conditions is a very tedious and complex task.

An HESS-based VSG is proposed in [21, 22] where inertia constant (H) and damping constant (D) are emulated and compared with conventional parameters. Here, conventional particle swarm optimization (PSO) is used for parameter optimization which suffers from several convergence challenges. Furthermore, a low pass filter-based approach is adopted for power sharing between battery and supercapacitor without considering frequency zenith which is caused by abrupt load shedding of power supply. In [23], NN-based variable fractional order PID (VFOPID) is proposed to address reduced inertia problem in isolated microgrid which is very computationally intensive considering online updating of parameters. Since the ultracapacitor and battery have different characteristics, it is very important to analyze them independently in order to design an HESS pack. Sizing of both battery and ultra-capacitor must be optimized in such a way that it is able to handle maximum change in energy demand while keeping the voltage and frequency within permissible limits.

Although determining the size of ultracapacitor and battery forming an HESS is a typical off-line optimization problem, but optimal utilization of their capacity for a given disturbance is an online optimization issue. Therefore, the controller gains must be updated while considering the amplitude of disturbance. A typical online optimization technique has been proposed in [24] where power fluctuations are handled by updating VSG variables using the backtracking search optimization approach. Here, the damping coefficient D is updated while taking RoCoF in account whereas inertia constant H is updated depending on frequency deviation. This technique exhibits superior performance in comparison to constant variable approach but at a higher computational cost. A similar approach based on self-adapting inertia and damping constant has been proposed in [25]. In [26], a fuzzy logic-based VSG has been proposed where the parameters are updated using change in power from RES and frequency deviation only while neglecting the RoCoF. Another fuzzy logic-based inertia control approach has been proposed in [27] where both the RoCoF and the frequency deviation have been considered for inertia updation. Since fuzzy logic-based approaches are expertise dependent, the effectiveness of such an algorithm depends on accuracy of rule formulation. The methodology described in reference [28] employs a bang-bang technique based virtual inertia calculation while considering damping coefficient as constant. A PSO-based methodology has been presented in [29] where low pass filter is used to determine the power sharing of HESS. However, low pass filter has inherent disadvantage of introducing delay which affects the control performance of the system. A PSO optimized fuzzy controller is proposed in [30, 31] which is found to be marginally better than the pure fuzzy-based approach. However, writing the rules for such a heavily fluctuating system is still a big issue.

Since RES-based microgrid is a highly volatile system, the gains of its proportional (Kp), integral (Ki), and derivative (Kd) controller (PID) regulator need to be updated as per the operating conditions. Determining the inertia gain under different operating conditions is a typical optimization problem for which lots of PSO-based methods have been reported as discussed previously. But the conventional PSO is having premature convergence issue which affects the control accuracy. Therefore, in the proposed work, an improvised version of the PSO approach has been implemented for the optimum adjustment of a PID regulator gain. Here, the improved PSO is a modified version of conventional PSO by incorporating natural exponential weight updating of velocity equation to avoid it from premature convergence. Furthermore, the optimal sizing of constituent component of HESS and effective utilization of their capacity in power sharing based on their response time improves the reliability of system at significantly lesser cost. The integral squared error (ISE) of frequency deviation is taken as an objective function for the tuning of PID regulator with the aim of enhancing rate of change of the frequency, zenith and nadir while minimizing the restoration time.

Here is a summary of this paper's main contribution:

- Application of improved PSO based PID controller on bidirectional DC–DC converter interfaced HESS to enhance frequency response in microgrid under severe disturbances to ensure system stability
- Automatically tuning of PID controller parameters based on both traditional PSO and improvised PSO in the novel adaptive virtual inertia control-based HESS
- Enhancement of frequency nadir, restoration time and RoCoF using improved PSO in comparison to conventional PSO tuned PID regulator.
- Optimal techniques applied to reduce the size of ultracapacitor-based HESS as a result of reduced restoration time, frequency nadir, and energy requirement.

This article is organized in five subdivisions first section as general introduction 1, second System Configuration of Virtual Inertia regulation. The third section has Proposed Virtual Inertia Control Concept for Frequency Regulation, the fourth section has Simulation and Experimental Results and discussion with setup validation. The conclusion is in the fifth section.

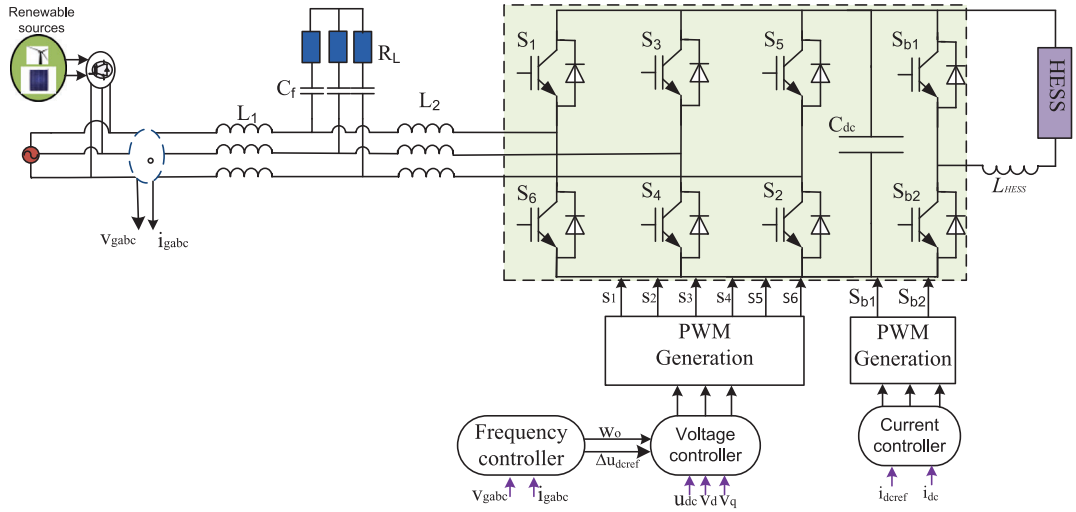

FIGURE 2 Schematic diagram of power converter in microgrid.

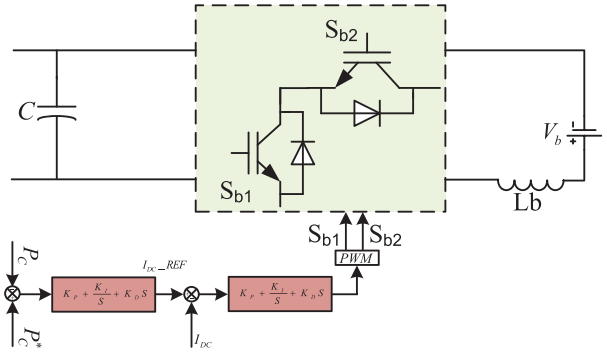

FIGURE 3 DC–DC bidirectional converter interface HESS diagram. HESS, hybrid energy storage system.

2 | SYSTEM CONFIGURATION AND CONTROL

Traditionally, synchronous generators are used to generate power and also to act as natural inertia and damping control. The turbine harnesses the stored kinetic energy to regulate the frequency. However, as renewable energy becomes more prevalent, the inherent inertia is diminishing. To accomplish this problem, the idea of VSG has been implemented [32]. In the proposed system as shown in Figure 2, a 15 MW photovoltaic (PV) generation unit (PVG), 200 mega volt amp (MVA) rated diesel generator unit (DG), wind power plant of 25 MW and battery/ultra-capacitor have been considered in the form of microgrid. Battery and ultracapacitor-based HESS has been considered to emulate the characteristics of VSG. HESS can offer active power regulation, energy management, and rapid and slow services in frequency control at a comparatively cheaper price [33]. The bidirectional DC–DC converter is used for coupling parallel combination of RRESS and SRESS to the DC-link of the grid interfacing inverter as seen in Figure 3. The common inverter uses virtual governor control similar to a traditional SG along with inertia and damping emulation as integral part of its control objectives. However, the power reference of RRESS also includes an energy recovery control. The RRESS's stored energy can be expressed as an SoC-equivalent value, such as $CV_{dc}^2/2$ for ultracapacitor.

The DC power transformation system (PTS) connected to the RRESS is responsible for maintaining DC voltage on the shared DC bus. However, the DC PTS of the SRESS is designed to adjust its power output based on the power reference from droop and integrated control loop, similarly to the turbine and governor system. Consequently, the RRESS autonomously delivers rapidly changing elements by controlling virtual inertia constants and damping constants. If the SRESS is designated as the slack bus, integral control may be used to restore the frequency. Consequently, the RRESS efficiently delivers the rapidly changing elements by effectively controlling virtual inertia and damping. The SRESS monitors the slow-fluctuating components of the VSG while detecting any changes in frequency.

In this paper, the parameters used were obtained from [34], and listed in Table 1.

2.1 | Energy variation and sizing of HESS due to frequency deviation

Sizing of ultra-capacitor is a crucial task when designing a virtual synchronous machine; it should be decided in such a way that maximum variation of energy during transient disturbance may be addressed. The greatest change in energy capacity is assessed by

$$\Delta E_{\max} = \frac{(E_{\max} - E_{nom}) + (E_{nom} - E_{\min})}{2} = E_{nom}\left(\frac{\Delta E_{\max}}{E_{nom}}\right) \quad (1)$$

By considering maximum energy changed due to frequency variation, J_{uc} inertia value which is emulated by ultra-capacitor gives; $\omega_{nom}, \omega_{zenith}$, and ω_{nadir} are nominal, zenith, and nadir frequencies respectively; and S_{rated} is the actual power of

TABLE 1 System descriptions and parameter values.

Features	Symbol	Value
Battery voltage	V_{b_ref}	350 V
Grid voltage	V_{g_ref}	415 V
DC inductance	$LHESS$	5.6 mH
DC link capacitance	C_{dc}	2.82 mF
DC-link voltage	$V_{C_{dc}}$	600 V
Frequency	f_{nom}	50 Hz
Turbine time coefficient	T_{Turb}	0.5 s
Governor time coefficient	T_{Gorvn}	0.2 s
Generator inertia coefficient	H	5 s
Governor speed regulation	$Rpermin$	0.05
Damping coefficient	D	0.8

ultra-capacitor.

$$\Delta E_{\max} = \frac{J_{uc}\left(w_{nom}^2 - w_{nadir}^2\right)}{2} or \frac{J_{uc}\left(w_{zenith}^2 - w_{nom}^2\right)}{2}$$

$$J_{uc} w_{nom} \Delta w_{\max} = \frac{J_{uc} w_{nom}^2}{2} \frac{\Delta w_{\max}}{w_{nom}} = H_{uc} S_{rated} \frac{\Delta w_{\max}}{w_{nom}} \quad (2)$$

Since Equations (1) and (2) are the same, therefore equating them will give

$$E_{nom} = \frac{H_{uc} S_{rated} \frac{\Delta w_{\max}}{w_{nom}}}{\frac{\Delta E_{\max}}{E_{nom}}} \quad (3)$$

For ultra-capacitor, maximum energy change is determined by

$$\Delta E_{\max} = \frac{\left(CV_{dc,\max}^2 - CV_{dc,nom}^2\right) + \left(CV_{dc,nom}^2 - CV_{dc,\min}^2\right)}{4}$$

$$= CV_{dc,nom} \Delta V_{dc,\max}/2 = CV_{dc,nom}^2 \times \left(\frac{\Delta V_{dc,\max}}{V_{dc,nom}}\right)/2 \quad (4)$$

To determine the size of the capacitor, Equations (3) and (4) are equated with the well-designed inertia constant H_{uc};

$$CV_{dc,nom}^2 \times \left(\frac{\Delta V_{dc,\max}}{V_{dc,nom}}\right)/2 = H_{uc} S_{rated} \frac{\Delta w_{\max}}{w_{nom}}$$
$$H_{uc} = \frac{C_{dc} V_{dc}^2}{2 S_{rated}} \cdot \frac{\Delta V_{dc\_\max} f_{nom}}{V_{dc} \Delta f_{\max}} \quad (5)$$

$$H_{uc} = H_{vi} \cdot \frac{\Delta V_{dc\_\max} f_{nom}}{V_{dc} \Delta f_{\max}} \quad (6)$$

where $H_{vi} = \frac{C_{dc} V_{dc}^2}{2 S_{rated}}$

As is seen in Equation (6), the factors to be considered for the virtual inertia constant (H_{uc}) are: given dc-link voltage V_{dc}, maximum ratio of voltage variation $\frac{\Delta V_{dc\_max}}{V_{dc}}$, minimum ratio of frequency variation $\frac{f_{nom}}{\Delta f_{\max}}$, and the rated dc-link capacitance C_{dc}.

Virtual inertia can be generated by designing a proportional controller as follows:

$$K_{vi} = \frac{\Delta V_{dc\_\max}}{V_{dc}} \cdot \frac{f_{nom}}{\Delta f_{\max}} \quad (7)$$

A proportional controller for allowable deviation of both frequency and voltage is indicated by MATLAB graph as shown in Figures 4a and 4b. The coding in MATLAB is done with the following values: The frequency change $\Delta f_{\max} = 0.2, \omega_{nom} = 50$ Hz, power rated was scaled down $S_{rated} = 1000$ VA, $\frac{\Delta V_{dc,\max}}{V_{dc,nom}} = 0.15$ and $C = 2.82$ mF [35].

As is seen in Figure 4a, for inertia of 5.03823 and voltage within the acceptable threshold of $400 \pm 36V$ (in this case 418.687 V), the capacitance needed is 333.333 μF. The available retails in capacitors can be found in market store. In Figure 4b, the change in voltage is restricted to 2.52525 V which is 5.3031% and is within the acceptable limits.

2.2 | Diesel generator

The governor of the SG controls the real power. The governor's main objective is to regulate the output power of diesel engine by adjusting the mechanical power of the synchronous generator to match the difference between mechanical and electrical power.

The swing equation is as follows in Equation (8):

$$\Delta P_m(t) - \Delta P_L(t) = \frac{2Hd\Delta f(t)}{dt} + D\Delta f(t) \quad (8)$$

where ΔP_m power production varies depending on the turbine

ΔP_L change power demand
Δf frequency deviation
H inertia constant
D damping constant

Equation (8) is represented in Figure 5.

Figure 6 shows the profile of how system frequency is controlled. In any network grid frequency is among the most crucial performance indicators. Frequency degradation of the system is due to abrupt disturbance caused by generation tripping or load shedding. Frequency is regulated to prevent large (RoCoF) and high-frequency deviation beyond allowable maximum.

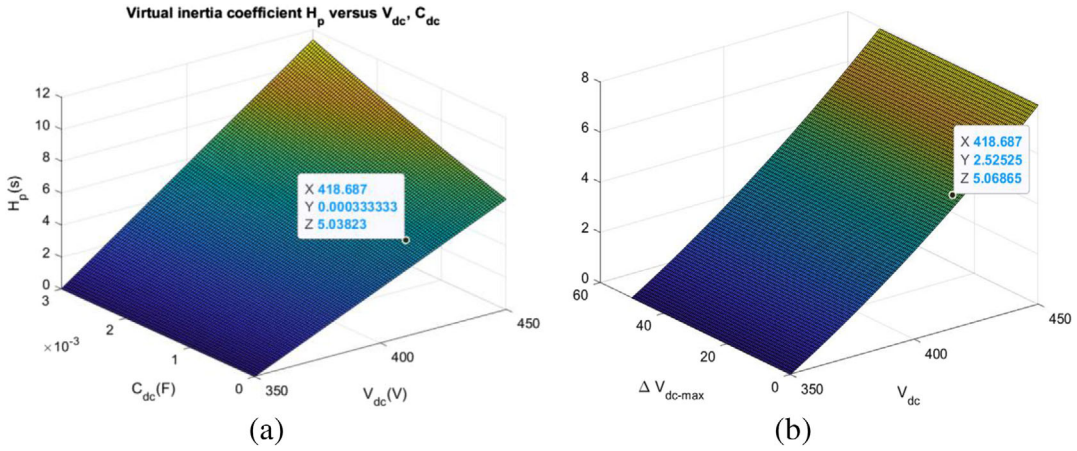

FIGURE 4 Virtual inertia coefficient (a) H_p versus $V_{dc,nom}$, C, (b) H_p versus $V_{dc,nom}$, $\Delta V_{dc,\max}$.

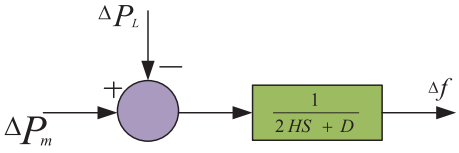

FIGURE 5 Frequency deviation model.

3 | PROPOSED VIRTUAL INERTIA CONTROL CONCEPT FOR FREQUENCY REGULATION

3.1 | Particle swarm optimization (PSO) implementation for PID controller parameters tuning

Control of HESS is essential to enhancing system stability. In this part, we will discuss how to regulate virtual inertia by determining ΔV_{dc} and Δf. This is done by utilizing a PID controller to acquire actual power reference. Here, an optimization technique is applied to automatic-tune the PID regulator. The improved PSO is a modified version of conventional PSO by incorporating natural exponential weight updating of velocity equation to avoid it from premature convergence. PSO was first introduced in 1995 by James Kennedy and Russel C. Eberhart [36]. It explains the social nature shown by animals, such as a group of birds and a group of fish. This technique is powerful, easy to implement, low computational burden, and efficient tool. It is suitable online optimization. The following formula determines the position and speed of each particle: local position p_i and best global position g_i of the particles are as follows:

$$d_i^{t+1} = d_i^t + u_i^{t+1} \tag{9}$$

$$u_i^{t+1} = wu_i^t + c_1 r_1 \left(p_i^t - d_i^t\right) + c_2 r_2 \left(g_i^t - d_i^t\right) \tag{10}$$

where r_1 and r_2 are random constant ranges (0 to 1)

c_1 and c_2 social coefficient and cognitive coefficient,
ω inertia weighting function
ωu_i^t inertia
$c_1 r_1 (p_i^t - d_i^t)$ cognitive unit
$c_2 r_2 (g_i^t - d_i^t)$ social unit

ω inertia weight, it is essential during exploitation and exploration in the search space. Well-optimized value reduces convergence period. In order to modify the inertia weight and update it dynamically, a highly successful method based on linearly decreasing inertia weight PSO was provided in reference [37] as given Equation (11).

$$w = (w_{start} - w_{end}) \times \left(\frac{T_{\max} - t}{T_{\max}}\right) + w_{end} \tag{11}$$

where ω_{start} is starting inertia weight

ω_{end} end value of inertia
$T_{\max}$ max iterations

During the searching procedure, the linear dynamic inertia weight-Particle Swarm Optimization (LDIW-PSO) encountered difficulty settling into a local optimum. Furthermore, excessively small or high values of the inertia constant may lead to an increase in the number of iterations and the time it takes for convergence, so negatively affecting the performance of the optimisation engine. In order to address this problem, we multiply the natural exponential with w_{end} to improve the equation for updating velocity, which was already introduced in our earlier publication paper [38]. Similarly, [39] have incorporated an exponential square, resulting in an additional rise in computation burden. To reduce computational burden while maintaining speed, a weight update matrix now includes an exponential component with an optimal value of $T_{\max}$ [40]. Consequently, the total time it takes for convergence lowers as the number of iterations is reduced. The adjusted Equation (12) has been modified

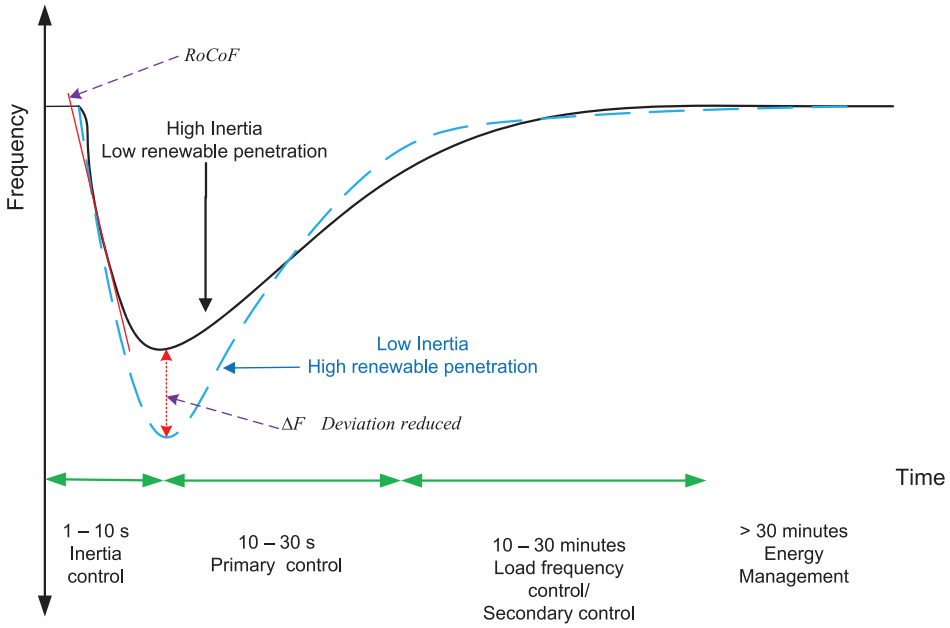

FIGURE 6 Main frequency deviation curve.

as follows:

$$w = (w_{start} - w_{end}) \times \left(\frac{T_{\max} - t}{T_{\max}}\right) + w_{end} \times e^{-t/\left(\frac{T_{\max}}{10}\right)} \quad (12)$$

where $w_{start} = 0.9$ and $w_{end} = 0.2$

The flowchart in Figure 7 is an algorithm for MPSO, modified inertia weight as inserted in Equations (10) and (12).

It is worth mentioning that the power required to maintain the frequency stability of the system may be determined by analysing the discrepancy between the voltage and normalized frequency. For adjustment and better frequency stability support, the PID controller is applied for correction in the differences [41], as stated in Equation (13), which is an extension of Equation (7), illustrating the achievement of reference active power.

$$P_{ref} = \left(\frac{\Delta f}{f_{nom}} - \frac{\Delta V}{V_{nom}}\right) \cdot \left(K_{P1} + \frac{K_{I1}}{S} + K_{D1}S\right) \quad (13)$$

In this proposed control strategy, power flows out from the ESS when there is increase in load or when a supply shuts down. When RES source is added, the power flows to the ESS. The converter acts as bidirectional virtual support. Virtual inertia control is critical for frequency stability as it reduces RoCoF and frequency zenith and nadir.

3.2 | Modelling of block diagrams of frequency control

The frequency control block is shown in the diagram, the frequency Q_g, f_g, and P_g are the measured grid reactive power, frequency, and real power respectively. The outcomes of the frequency control are displacement angle θ_o, output frequency f_o, and angular frequency ω_o. The controller operates in a similar manner as standard frequency controller of synchronous generators [42]. Figure 8 shows switching signals which control the gates. The frequency control diagram is shown in Figure 9.

4 | ANALYSIS OF SIMULATION AND EXPERIMENTAL FINDINGS AND DISCUSSION

4.1 | Simulation findings and discussion

The effectiveness of the proposed technique was evaluated by simulating the frequency of the microgrid using Matlab/Simulink. The ultracapacitor is designed to improve frequency responsiveness. Parameter tuning is done by the use of optimization techniques. As shown, frequency deviation Δf is the optimal objective function,

$$ISE = \int_0^{T_{Sim}} |\Delta f^2| dt \quad (14)$$

where

ISE is integral squired error
T_{Sim} is simulation time range

The objective function in Equation (14) is applied using both optimization techniques and the outcomes are recorded in Table 2. In performance index ISE, the error is squared; therefore, it handles both positive and negative errors.

The cases considered in the analysis of this proposed controller in the MG's frequency response are as follows:

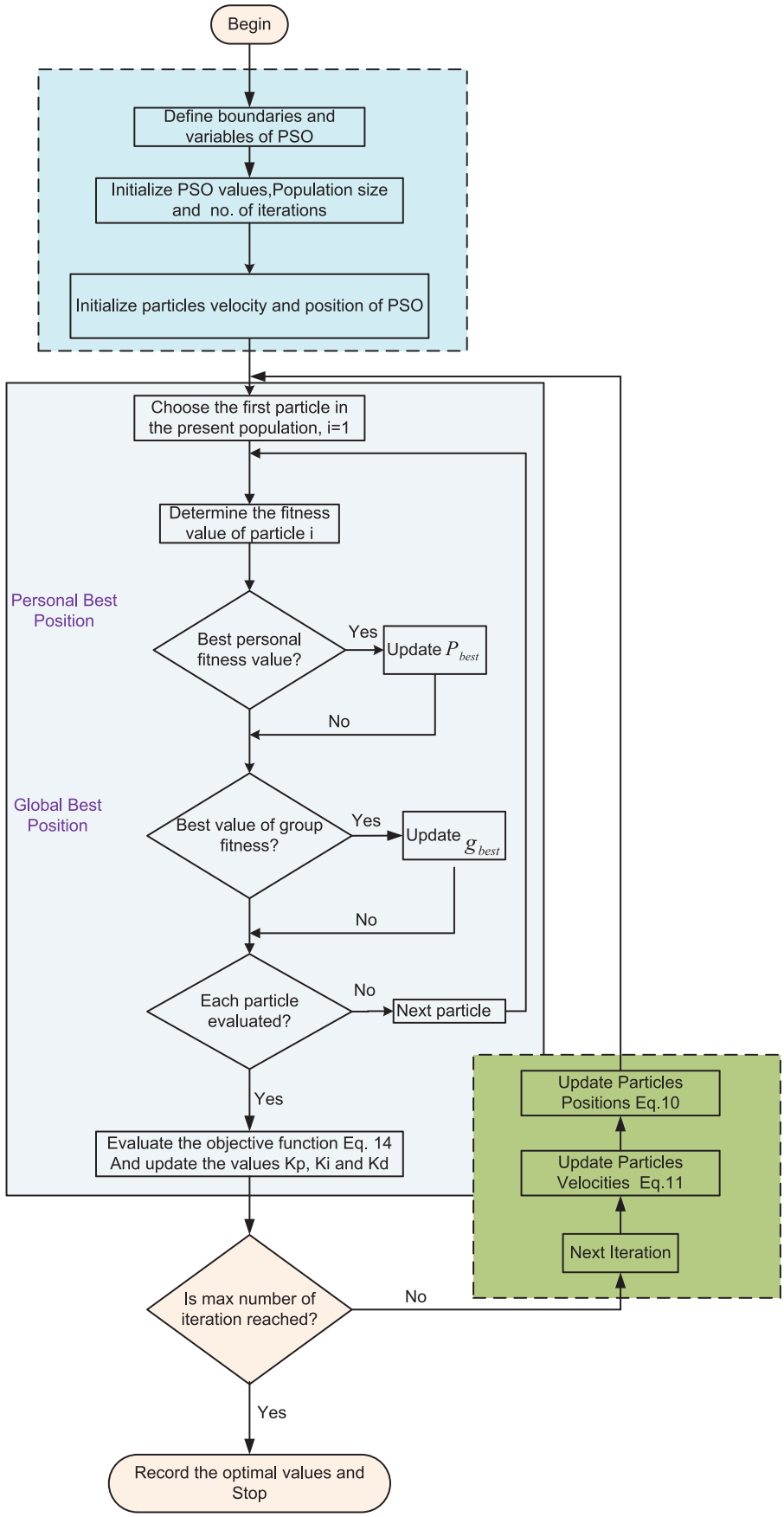

FIGURE 7 Improved particle swarm optimization (MPSO) flowchart.

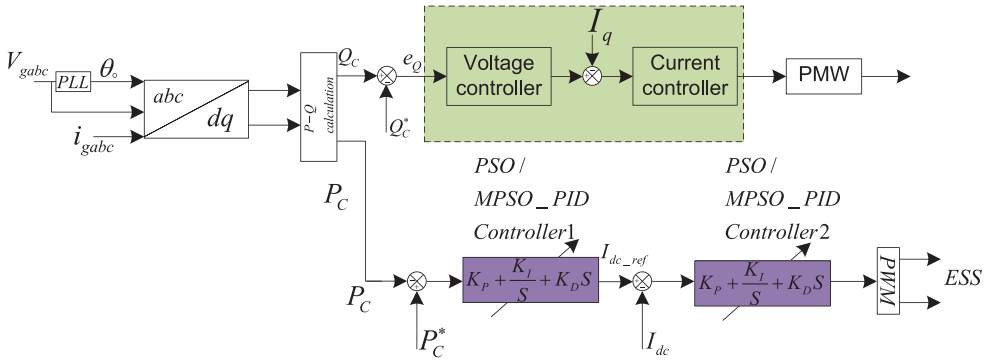

FIGURE 8 Block diagrams of control frame for switching signals.

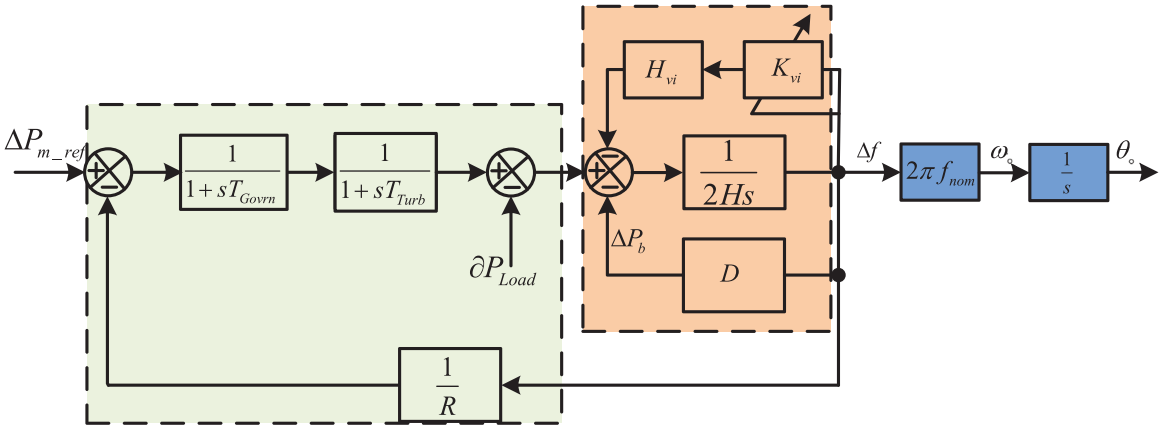

FIGURE 9 Block diagram of inertia control structure of frequency regulation.

TABLE 2 Optimal values.

Parameters	PSO	Improved PSO
K_P	1000	1000
K_I	39.0995	0.6893
K_D	0	0

Abbreviation: PSO, particle swarm optimization.

CASE 1: Increased power generation of 5 MW from PV

Figure 10a illustrates the frequency response of microgrid due sudden increase in PV generated power at 0.2 s by virtue of increased radiations. The frequency rose abruptly post disturbance attributed to power generated by PV unit. Both the convectional PSO and Improved PSO have been implemented for parameters tuning in such a way that the deviation in frequency is contained within the permissible threshold. However, Improved PSO has smaller frequency deviation compared with conventional PSO; that is, 50. 0199 Hz and 50.997, respectively. The difference in frequencies is used to calculate the capacity of ultracapacitor energy saved by applying Equation (2). The difference in frequencies using both the methods is found to be 0.98 Hz which is equivalent to additional amount of energy storage of 490 kW.s. needed to curtail the frequency deviation. In other words, the improvised PSO helps in reducing the additional storage capacity in comparison to conventional PSO.

CASE 2: Increase in load demand of 7.5 MW

In this scenario, a sudden surge in load demand of 7.5 MW is considered at 3 s. Due to this disturbance, frequency drop is seen just after the increase in load as depicted in Figure 11a. In this scenario, the lowest point is 48.52 Hz using conventional PSO, though it is within allowable frequency deviation but it requires large ultracapacitor to accommodate the fluctuation of such magnitude. For improved PSO, the frequency deviation is found to be 49.97 Hz. The difference between the two strategies in terms of frequency is 1.45 Hz. Thus, by applying Equation (2), the additional storage capacity of 1.0875 MW.s is saved using proposed Improvised PSO. For the convenience of comparison, the disturbance for scenario 1 was kept constant throughout the simulation at 0.2 of 5 MW.s. Furthermore, the fact that this technique can handle both circumstances at once is proof that it is better.

CASE 3: Increase in wind generated power of 10 MW

In this scenario, a sudden enhanced wind power of 10 MW is considered at 6 s due to sudden increase in wind velocity. Due to this sudden increase, imbalance between demand and supply arises which results in frequency shoot up as shown in Figure 12a. The highest point is 51.9886 Hz based on PSO and 50.0398 Hz based on Improved PSO. It is to be noticed that the

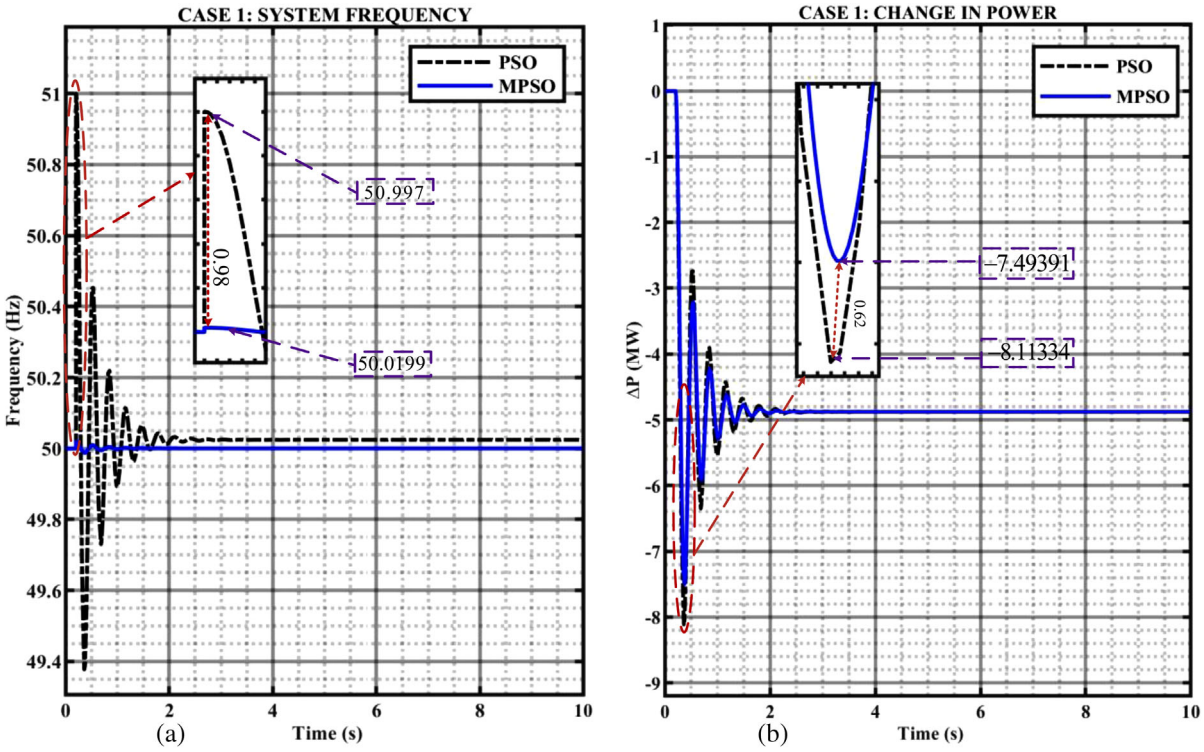

FIGURE 10 (a) Frequency response, (b) 5 MW increased power generation of 5 MW from PV.

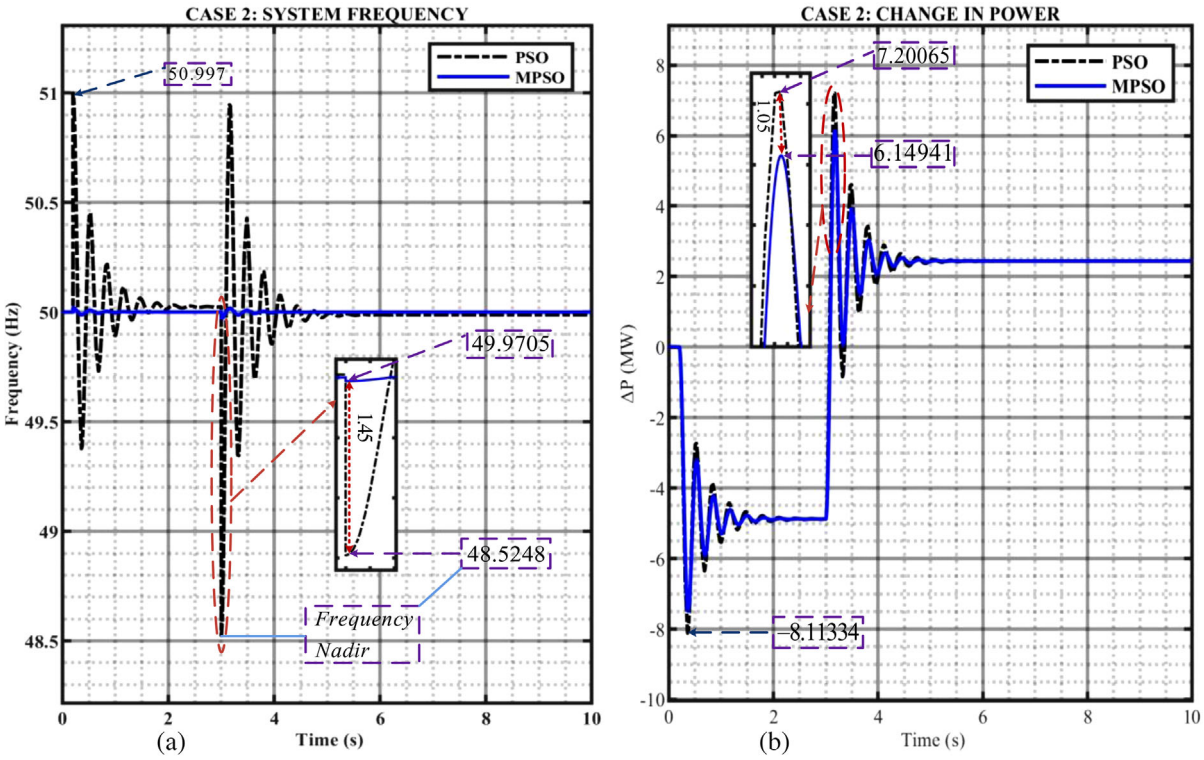

FIGURE 11 (a) Frequency response. (b) Increase in load demand of 7.5 MW.

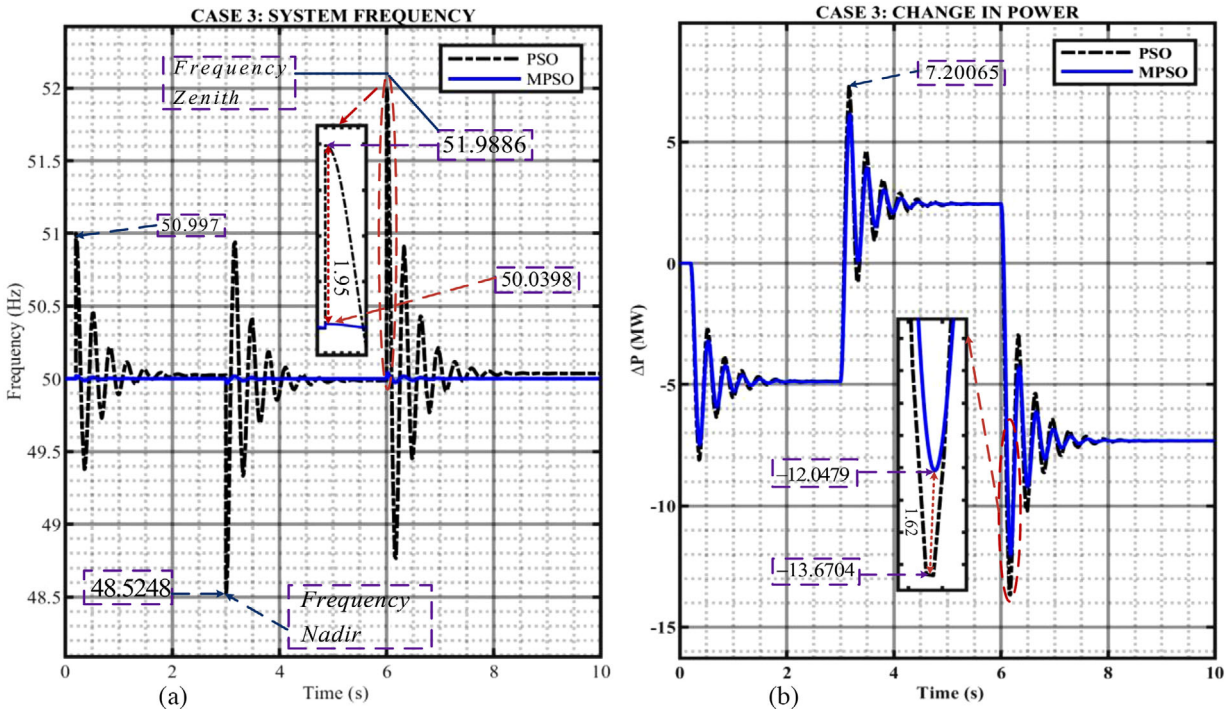

FIGURE 12 (a) Frequency response. (b) Increase in wind generated power of 10 MW.

TABLE 3 Microgrid frequency deviations.

	Frequency deviation (Hz)	
Case	**Convectional PSO**	**Improved PSO**
1	0.997	0.0199
2	1.4752	0.0295
3	1.9886	0.0398

Abbreviation: PSO, particle swarm optimization.

differences in frequency using both the strategies are 1.95 Hz. The energy calculated for this much frequency difference is of 1.95 MW.s. This shows that the cost of installing larger ultracapacitor is reduced with Improved PSO. To make comparisons simple, disturbances for Case 1 at 0.2 s of 5 MW and Case 2 at 3 s of 7.5 MW were included during simulation. Given that it can manage all three eventualities at once, this technique provides further proof of its superiority. The results of the simulations show that frequency is restored in every instance.

From Table 3, are tabulated results of the simulation of the microgrid frequency deviation. It was conducted in all test conditions. The findings clearly demonstrate that the proposed controller outperformed the convectional method. The proposed method is ensuring frequency stabilization and economical use of ultracapacitor. Here, it could be observed that for a minimum disturbance of 5 MW, the change in frequency is

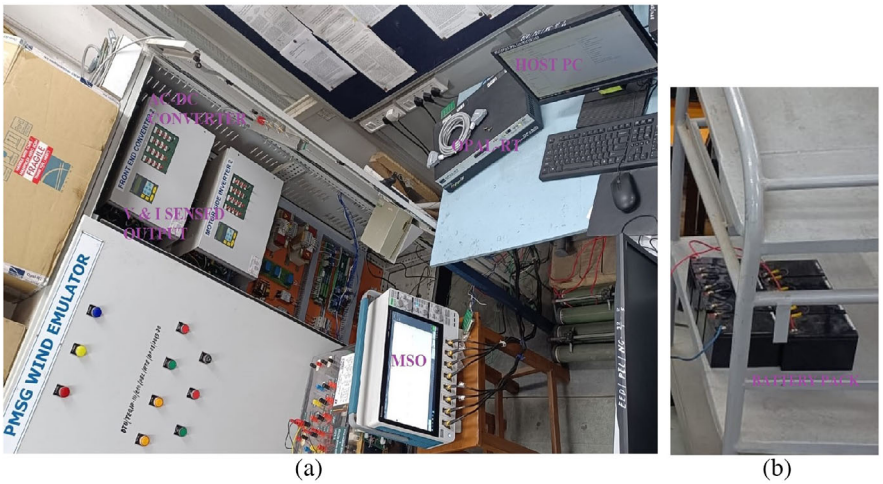

FIGURE 13 Photo of experimental setting. (a) Setup. (b) Battery pack.

TABLE 4 Sum up of the frequency response under various severe disturbances.

	Disturbance	Frequency response
Load fluctuation	Load increasing	Decrease (nadir)
	Load shedding (decreasing)	Increase (zenith)
Wind speed variation	Speed increment	Increase (zenith)
	Speed decrement	Decrease (nadir)
Solar irradiation variation	Radiations increment	Increase (zenith)
	Radiations decrement	Decrease (nadir)
Contingency	RES disconnecting	Decrease (nadir)
	RES connecting	Increase (zenith)

0.997 (1.994 %) while with Improved PSO frequency change is 0.0199 (0.0398%). Similarly with a maximum disturbance of 10 MW, the change in frequency is 1.9886 (3.977%) while Improved PSO yields a frequency change of 0.0398 (0.0796%). Thus, it is evident from the two extreme cases that with Improved PSO the change in frequency is very small. For brevity purposes, Table 4 is a summary of frequency response in a microgrid under different disturbance scenarios.

4.2 | Experimental results and discussion

The simulation study carried out in the MATLAB/Simulink environment is validated in real time using (OP-4510) OPAL-RT as demonstrated in Figure 13. This offers as further evidence of the effectiveness of the proposed study concept in a real-time setting.

The fast dynamic response of the proposed dynamic controller is apparent; it is capable of quickly reducing the frequency deviation in under 2 s, regardless of the degree of the disturbance. In the experimental study, disturbances of 2%, 3%, and 4% were introduced and it can be observed that the response times in all three situations a found to be very quick. The

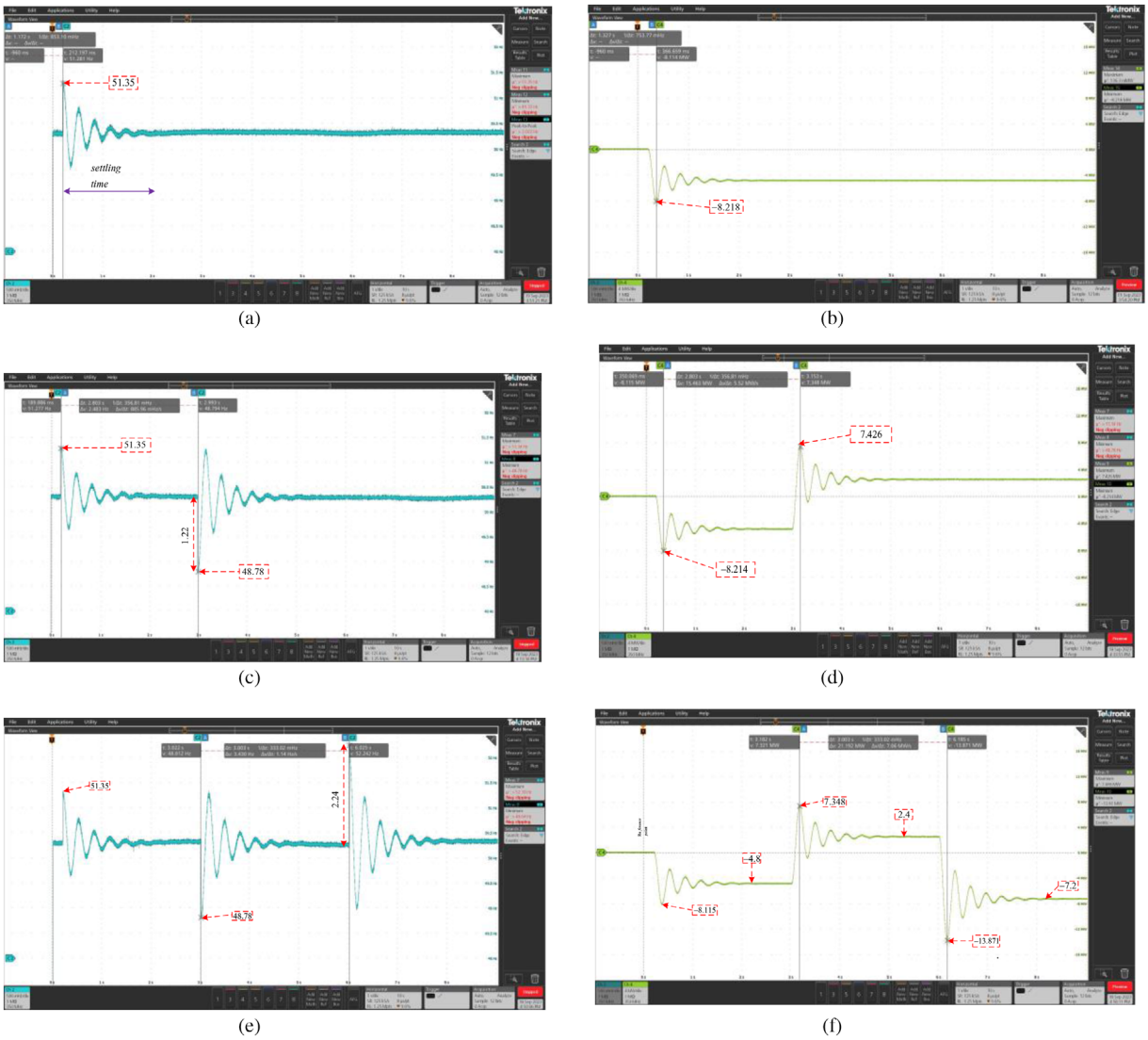

FIGURE 14 Frequency deviation (a) 5 MW, (c) 7.5 MW, (e) 10 MW. Power change (b) 5 MW, (d) 7.5 MW, (f) 10 MW.

TABLE 5 Distinction of proposed control technique over other methods.

Reference	Type of a controller	Contribution
[43]	Hybrid ESS based on heuristics methods	PID controller parameters are tuned using GA and PSO but suffers local optima problem
[29]	Optimal virtual synchronous generator control of HESS	Designing optimal VSG using PSO but suffers local optima and frequency oscillations take long to settle
[44]	PID controller based on the Grey Wolf Optimization (GWO) algorithm	Frequency regulation in the microgrid designed for a multi-source single-area system; however, it does not take into account multiple areas or the impact of (RES).
[45]	BFOA tuned LQR-based VSG	Suppress frequency variations using robust design strategies. It suffers convergence challenge.
Proposed	HESS based on improved PSO	Optimizing PID controller settings using an enhanced version of PSO and traditional PSO. The Improved PSO algorithm is online optimization technique which successfully addressed the difficulties of local optima and lengthen iterations.

Abbreviations: BFOA, bacteria foraging optimization algorithm; HESS, hybrid energy storage system; LQR, linear-quadratic regulator; PID, proportional (Kp), integral (Ki), and derivative (Kd) controller; PSO, particle swarm optimization; VSG, virtual synchronous generators.

results from the real-time OPAL-RT (OP-4510) and MATLAB simulations are consistent, indicating that offline systems may employ the adjusted optimum PID controller parameters. This is done to support the suggested control strategy, which virtually emulates simulation results with hardware in loop.

As seen in Figures 14a to f, the same three cases have been implemented using HIL. It is worthwhile noting that with disturbance in load operating conditions, the disturbance in frequency is restored as per grid code requirements. Moreover, the restoration period using the proposed method is found to be very much smaller in comparison to conventional methods which further results in an enhanced stability.

Finally, a brief comparison and distinction with the existing state-of-the-art methods of control in grid-connected ESSs have been provided in Table 5.

5 | CONCLUSION

In this paper, frequency stabilization of RESs based low inertia microgrid has been achieved with HESS. The optimal sizing of HESS is done in such a way that it utilizes the response characteristics of Ultracapacitor and battery in order to have enhanced performance with reduced cost. Ultracapacitor is used to mimic inertia for high frequency power deviation as seen during simulation, whereas battery is applied for long-term power variation in microgrid. A modified form of particle swarm optimization was used to optimize the PID factors. The efficiency of the proposed control strategy has been proved by examining three distinct levels of uncertainty generated by either intermittent RESs or changing load. There has been a considerable decrease in the problems related to the rate of change of frequency, overshoot, undershoot, and rising time. As a result, the required size of ultracapacitors has been reduced. In turn, the cost of the entire system is reduced. The effectiveness of modified particle swarm optimization is evident when comparing it to traditional particle swarm optimization. It is worthy to note that there is significant amount of energy saving capacity of 1. 95 MW.s for a disturbance of 10 MW. Moreover, the conventional particle swarm optimization technique yielded a frequency deviation of 1.9886 Hz, but the proposed Improved particle swarm optimization technique successfully decreased it to 0.0398 Hz. Therefore, the suggested method enhances the overall efficiency of the microgrid across various operational scenarios. The simulation findings, together with the experimental findings, confirm the efficacy of the proposed strategy in terms of determining the appropriate size of the Hybrid Energy Storage System (HESS) and enhancing the control performance of the Microgrid. The future investigation should consider seamless power sharing in HESS and the ratios based on online optimization.

AUTHOR CONTRIBUTIONS

Philemon Yegon: Conceptualization; data curation; formal analysis; investigation; methodology; software. **Mukhtiar Singh**: Supervision; validation; visualization; writing—review & editing.

CONFLICT OF INTEREST STATEMENT

The authors declare no conflicts of interest.

FUNDING INFORMATION

No funding has been received from any source for the implementation of this research. This research work is entirely the product of authors' initiatives.

DATA AVAILABILITY STATEMENT

The data that support the findings of this study are available from the corresponding author upon request.

ORCID

Philemon Yegon https://orcid.org/0009-0003-3179-1511

REFERENCES

1. Fang, J., Li, H., Tang, Y., Blaabjerg, F.: On the inertia of future more-electronics power systems. IEEE J. Emerg. Sel. Top. Power Electron. 7(4), 2130–2146 (2019). https://doi.org/10.1109/JESTPE.2018.2877766
2. Chang-Chien, L.R., An, L.N., Lin, T.W., Lee, W.J.: Incorporating demand response with spinning reserve to realize an adaptive frequency restoration plan for system contingencies. IEEE Trans. Smart Grid 3(3), 1145–1153 (2012). https://doi.org/10.1109/TSG.2012.2192297
3. Liu, K., Qu, Y., Kim, H.M., Song, H.: Avoiding frequency second dip in power unreserved control during wind power rotational speed recovery. IEEE Trans. Power Syst. 33(3), 3097–3106 (2018). https://doi.org/10.1109/TPWRS.2017.2761897
4. ISO 2013: Reciprocating internal combustion engine driven alternating current generating sets — Part 5: Generating sets. 2013. https://cdn.standards.iteh.ai/samples/81844/3dd696ded80349f29547ba03decd6705/ISO-8528-5-2022.pdf

5. NERC: Frequency Response Initiative Report. 2012. https://www.nerc.com/pa/Stand/Project200712FrequencyResponseDL/Bal-003-1-Background_Document-Clean-2013_FILING.pdf
6. Huang, L., Xin, H., Wang, Z.: Damping low-frequency oscillations through VSC-HVdc stations operated as virtual synchronous machines. IEEE Trans. Power Electron. 34(6), 5803–5818 (2019). https://doi.org/10.1109/TPEL.2018.2866523
7. Soni, N., Doolla, S., Chandorkar, M.C.: Inertia design methods for islanded microgrids having static and rotating energy sources. IEEE Trans. Ind. Appl. 52(6), 5165–5174 (2016). https://doi.org/10.1109/TIA.2016.2597281
8. Yuan, C., Yang, D., Feng, J., Liu, C.: Constrained operation zone of a VSG considering the DC-side power margin. J. Eng. 2019(16), 2563–2568 (2019). https://doi.org/10.1049/joe.2018.8679
9. Meng, J., et al.: An overview and comparison of online implementable SOC estimation methods for lithium-ion battery. IEEE Trans. Ind. Appl. 54(2), 1583–1591 (2018). https://doi.org/10.1109/TIA.2017.2775179
10. Ma, Y., Cao, W., Yang, L., Wang, F.F., Tolbert, L.M.: Virtual synchronous generator control of full converter wind turbines with short-term energy storage. IEEE Trans. Ind. Electron. 64(11), 8821–8831 (2017). https://doi.org/10.1109/TIE.2017.2694347
11. Sun, C., Ali, S.Q., Joos, G., Bouffard, F.: Design of hybrid-storage-based virtual synchronous machine with energy recovery control considering energy consumed in inertial and damping support. IEEE Trans. Power Electron. 37(3), 2648–2666 (2022). https://doi.org/10.1109/TPEL.2021.3111482
12. Chapaloglou, S., Alves, E.F., Trovato, V., Tedeschi, E.: Optimal energy management in autonomous power systems with probabilistic security constraints and adaptive frequency control. IEEE Trans. Power Syst. 39(1), 1543–1554 (2024). https://doi.org/10.1109/TPWRS.2023.3236378
13. Bhattar, C.L., Chaudhari, M.A.: Centralized energy management scheme for grid connected DC microgrid. IEEE Syst. J. 17(3), 3741–3751 (2023). https://doi.org/10.1109/JSYST.2022.3231898
14. Ikram, A.I., Ullah, A., Datta, D., Islam, A., Ahmed, T.: Optimizing energy consumption in smart homes: Load scheduling approaches. IET Power Electron. 2023, 1–13 (2024). https://doi.org/10.1049/pel2.12663
15. Chen, Y., Meng, J., Yan, Y., Zhong, L.: Quasi-Z based adaptive sliding mode control for three-phase photovoltaic grid-connected system. IET Power Electron. 16(15), 2577–2591 (2023). https://doi.org/10.1049/pel2.12584
16. Majeed, M.A., Phichisawat, S., Asghar, F., Hussan, U.: Optimal energy management system for grid-tied microgrid: An improved adaptive genetic algorithm. IEEE Access 11, 117351–117361 (2023). https://doi.org/10.1109/ACCESS.2023.3326505
17. Joshi, M.C., Samanta, S.: Energy management with improved frequency sharing based control for battery/ultracapacitor hybrid energy system in the presence of delay. IET Power Electron. 13(10), 2019–2028 (2020). https://doi.org/10.1049/iet-pel.2018.5118
18. Maleki, S., Nikoukar, J., Tousifian, M.H.: Robust frequency control of microgrids: A mixed H2/H∞ virtual inertia emulation. Int. Trans. Electr. Energy Syst. 2023, 1 (2023). https://doi.org/10.1155/2023/6872765
19. Golpîra, H., Seifi, H., Messina, A.R., Haghifam, M.R.: Maximum penetration level of micro-grids in large-scale power systems: Frequency stability viewpoint. IEEE Trans. Power Syst. 31(6), 5163–5171 (2016). https://doi.org/10.1109/TPWRS.2016.2538083
20. Guo, L., Xu, Z., Jin, N., Li, Y., Wang, W.: A weighted voltage model predictive control method for a virtual synchronous generator with enhanced parameter robustness. Prot. Control Mod. Power Syst. 6(1), 1–11 (2021). https://doi.org/10.1186/s41601-021-00217-8
21. Elwakil, M.M., Zoghaby, H.M.E., Sharaf, S.M., Mosa, M.A.: Adaptive virtual synchronous generator control using optimized bang-bang for Islanded microgrid stability improvement. Prot. Control Mod. Power Syst. 8(1), 57 (2023). https://doi.org/10.1186/s41601-023-00333-7
22. Shi, T., Sun, J., Han, X., Tang, C.: Research on adaptive optimal control strategy of virtual synchronous generator inertia and damping parameters. IET Power Electron 17(1), 121–133 (2024). https://doi.org/10.1049/pel2.12620
23. Skiparev, V., et al.: Virtual inertia control of isolated microgrids using an NN-based VFOPID controller. IEEE Trans. Sustain. Energy 14(3), 1558–1568 (2023). https://doi.org/10.1109/TSTE.2023.3237922
24. Leng, D., Polmai, S.: Virtual synchronous generator based on hybrid energy storage system for PV power fluctuation mitigation. Appl. Sci. 9(23), 1–18 (2019). https://doi.org/10.3390/app9235099
25. Li, D., Zhu, Q., Lin, S., Bian, X.Y.: A self-adaptive inertia and damping combination control of VSG to support frequency stability. IEEE Trans. Energy Convers. 32(1), 397–398 (2017). https://doi.org/10.1109/TEC.2016.2623982
26. Kerdphol, T., Watanabe, M., Hongesombut, K., Mitani, Y.: Self-adaptive virtual inertia control-based fuzzy logic to improve frequency stability of microgrid with high renewable penetration. IEEE Access 7, 76071–76083 (2019). https://doi.org/10.1109/ACCESS.2019.2920886
27. Hu, Y., Wei, W., Peng, Y., Lei, J.: Fuzzy virtual inertia control for virtual synchronous generator. In: Chinese Control Conference CCC 2016, Aug., pp. 8523–8527 (2016). https://doi.org/10.1109/ChiCC.2016.7554718
28. Alipoor, J., Miura, Y., Ise, T.: Power system stabilization using virtual synchronous generator with alternating moment of inertia. IEEE J. Emerg. Sel. Top. Power Electron. 3(2), 451–458 (2015). https://doi.org/10.1109/JESTPE.2014.2362530
29. Mohamed, M.M., El Zoghby, H.M., Sharaf, S.M., Mosa, M.A.: Optimal virtual synchronous generator control of battery/supercapacitor hybrid energy storage system for frequency response enhancement of photovoltaic/diesel microgrid. J. Energy Storage 51, 104317 (2022). https://doi.org/10.1016/j.est.2022.104317
30. Chong, L.W., Wong, Y.W., Rajkumar, R.K., Isa, D.: An optimal control strategy for standalone PV system with battery-supercapacitor hybrid energy storage system. J. Power Sources 331, 553–565 (2016). https://doi.org/10.1016/j.jpowsour.2016.09.061
31. Le Nguyen, V.T.N.T.B.: Stability analysis of an isolated microgrid with the presence of the hybrid energy storage system-based virtual synchronous generator. J. Sci. Technol. Issue Inf. Commun. Technol. 46–51 (2020). https://doi.org/10.31130/jst-ud2020-101e
32. Li, K., Cheng, P., Wang, L., Tian, X., Ma, J., Jia, L.: Improved active power control of virtual synchronous generator for enhancing transient stability. IET Power Electron. 16(1), 157–167 (2023). https://doi.org/10.1049/pel2.12371
33. Oh, Y.G., Kwon, O., Kwon, J.M.: Bidirectional push–pull/H-bridge converter for low-voltage energy storage system. IET Power Electron. 17(1), 1–9 (2024). https://doi.org/10.1049/pel2.12586
34. Saadat, H. Power System Analysis. McGraw Hills-COMPANIES, New York (1999). https://doi.org/10.1201/9781003394433-4
35. Fang, J., Li, H., Tang, Y., Blaabjerg, F.: Distributed power system virtual inertia implemented by grid-connected power converters. IEEE Trans. Power Electron. 33(10), 8488–8499 (2018). https://doi.org/10.1109/TPEL.2017.2785218
36. James Kennedy, R.E.: Particle swarm optimization. In: Proceedings of ICNN'95 - International Conference on Neural Networks, Perth, WA, Australia, pp. 1942–1948 (1995). https://doi.org/10.1109/ICNN.1995.488968
37. Arasomwan, M.A., Adewumi, A.O.: On the performance of linear decreasing inertia weight particle swarm optimization for global optimization. Sci. World J. 2013, 1–12 (2013). https://doi.org/10.1155/2013/860289
38. Yegon, P., Singh, M.: Frequency stability enhancement of microgrid using optimization techniques-based adaptive virtual inertia control. Int. Trans. Electr. Energy Syst. 2023, 1 (2023). https://doi.org/10.1155/2023/2121721
39. Oladipo, S., Sun, Y., Adeleke, O.: An improved particle swarm optimization and adaptive neuro-fuzzy inference system for predicting the energy consumption of university residence. Int. Trans. Electr. Energy Syst. 2023, 1 (2023). https://doi.org/10.1155/2023/8508800
40. Guimin, C., Xinbo, H., Jianyuan, J., Zhengfeng, M.: Natural exponential inertia weight strategy in particle swarm optimization. Proc. World Congr. Intell. Control Autom. 1(2002), 3672–3675 (2006). https://doi.org/10.1109/WCICA.2006.1713055
41. Zhang, Z., Fang, J., Dong, C., Jin, C., Tang, Y.: Enhanced grid frequency and DC-link voltage regulation in hybrid AC/DC microgrids through

bidirectional virtual inertia support. IEEE Trans. Ind. Electron. 70(7), 6931–6940 (2023). https://doi.org/10.1109/TIE.2022.3203757
42. Kundur, P. Power System Stability and Control. McGraw Hill Education (2007). https://doi.org/10.1201/9781420009248
43. Guentri, H., Allaoui, T., Mekki, M., Denai, M.: Power management and control of a photovoltaic system with hybrid battery-supercapacitor energy storage based on heuristics methods. J. Energy Storage 39, 102578 (2021). https://doi.org/10.1016/j.est.2021.102578
44. Paliwal, N., Srivastava, L., Pandit, M.: Application of grey wolf optimization algorithm for load frequency control in multi-source single area power system. Evol. Intell. 15(1), 563–584 (2022). https://doi.org/10.1007/s12065-020-00530-5
45. Singh, S.K., Singh, R., Ashfaq, H., Kumar, R.: Virtual inertia emulation of inverter interfaced distributed generation (IIDG) for dynamic frequency stability & damping enhancement through BFOA tuned optimal controller. Arab. J. Sci. Eng. 47(3), 3293–3310 (2022). https://doi.org/10.1007/s13369-021-06121-5

How to cite this article: Yegon, P., Singh, M.: Optimization of battery/ultra-capacitor hybrid energy storage system for frequency response support in low-inertia microgrid. IET Power Electron. 1–15 (2024). https://doi.org/10.1049/pel2.12723